 doi:10.20944/preprints202109.0368.v2

Black Holes as Markers of Dimensionality

Szymon Łukaszyk *

Black hole temperature $T_{BH} = T_P/2\pi d$ as a function of its Planck length real diameter multiplier d is derived from black hole surface gravity and Hawking temperature w.l.o.g. It is conjectured $d = 1/2\pi$ describes primordial Big Bang singularity as in this case $T_{BH} = T_P$. A black hole interacts with the environment and observable black holes have uniquely defined Delaunay triangulations with a natural number of spherical triangles having Planck areas (bits), where a Planck triangle is active and has gravitational potential of $-c^2$ if all its vertices have black hole gravitational potential of $-c^2/2$ and is inactive otherwise. As temporary distribution of active triangles on an event horizon tends to maximize Shannon entropy a black hole is a fundamental, one-sided thermodynamic equilibrium limit for a dissipative structure. Black hole blackbody radiation, informational capacity fluctuations, and quantum statistics are discussed. On the basis of the latter, wavelength bounds for BE, MB, and FD statistics are derived as a function of the diameter multiplier d. It is shown that black holes feature wave-particle duality only if $d \leq 8\pi$, which also sets the maximum diameter of a totally collapsible black hole. This outlines the program for research of other nature phenomena that emit perfect blackbody radiation, such as neutron stars and white dwarfs.

Keywords: quantum black holes, entropic gravity; the black hole information paradox; Shannon entropy; Delaunay triangulation; black hole quantum statistics; logistic function/map; exotic $\mathbb{R}^4$

1. Introduction

The combinatorial proof of the *H*-theorem [1] that Ludwig Boltzmann derived in 1877 introduced energy quantization. This led to the development of quantum theory [2] and brought about to the problem of measurement, performed *hic et nunc* by any particular observer, yielding rational information. This information is twofold; it relates both to *without* of things, as well as to *within* of things; quoting Pierre Teilhard de Chardin "In the eyes of the physicist, nothing exists legitimately, at least up to now, except the *without* of things. The same intellectual attitude is still permissible in the bacteriologist, whose cultures (apart from some substantial difficulties) are treated as laboratory reagents. But it is already more difficult in the realm of plants. It tends to become a gamble in the case of a biologist studying the behavior of insects or coelenterates. It seems merely futile with regard to the vertebrates. Finally, it breaks down completely with man, in whom the existence of a *within* can no longer be evaded, because it is the object of a direct intuition and the substance of all knowledge" [3].

2. Dimensionalities

Dimensionalities of the *within* (the interior) and the *without* (the exterior) of things are researched in this paper. Any *n*-dimensional interior is bounded by (*n*-1)-dimensional topological sphere as asserted by the Jordan-Brouwer separation theorem. However, a black hole is an exception: unbounded black hole exterior has a boundary (event horizon) but a black hole does not have a bounded interior. Therefore black hole invalidates not only the Jordan-Brouwer separation theorem but also the generalized Stokes theorem: a differential form over the black hole event horizon is not equal to the integral of its exterior derivative over the black hole interior. There is no such thing as the black hole interior.

Author shares the *it from bit* John Archibald Wheeler conclusion, yet is of the opinion that his statement that "there is no such thing at the microscopic level as space or time or spacetime continuum" [4] remains valid at any level, not only microscopic. Thus nature should be researched as a vertex-labeled graph (graph of nature) having certain intrinsic properties reflecting the 2nd law of thermodynamics. Primordial Big Bang singularity (the first point or vertex) expanded the graph of nature into dimensionalities [5] not into a 4-dimensional spacetime.

It is assumed in this paper that dimension n is a complex number, wherein biological evolution is possible only in dimension $n = 3 + i$ with 3 spatial dimensions and imaginary time due to the exotic $\mathbb{R}^4$ property of such a space [5]. In fact the only real imaginary number is $0i = 0$. This zero is the *nunc*, the moment that passes for every living biological cell. It cannot be just put outside the realm of science [6, 7, 8]. Hence Lorentz transformations are rotations of the 4-ball of a fixed radius R

$$x^2 + y^2 + z^2 + (ict)^2 = R^2 . \quad (1)$$

For an information to be transmitted between the *without* and the *within* the factors (1, 1, 1, 1) in $n = 3 + i$ must be unit lengths and this transmission takes place through $(2 + i)$-dimensional topological bounding sphere.

Dimension of a space is usually defined as the minimum number of independent parameters (coordinates) needed to specify a point within this space. Since a point in a fractionally dimensional space cannot be unambiguously defined within this space, such a point cannot be observed. Such fractional dimensionalities remain *latent* (=hidden, but present) [1] [9]. Fractals feature fractional dimensionalities but it is impossible to *observe* the whole fractal in the *nunc*; fractional dimensionality of a fractal is present only in a recurrence relation that defines it. Furthermore most fractals are nowhere differentiable, which links them with the exotic $\mathbb{R}^4$ property required for biological evolution [5].

It is known that spaces with natural and low dimensionalities are the most interesting: Fermat's Last Theo-

* szymon@patent.pl

[1] For humans latent dimensionalities obviously also include $n < -1$ and $n > 3$.

Preprints (www.preprints.org) | NOT PEER-REVIEWED | Posted: 25 November 2021 doi:10.20944/preprints202109.0368.v2

rem indicates the importance of $n = \{1, 2\}$; $n = 4$ models spacetime, maximizes the number (six) of regular polytopes (excluding $n = 2$) and has the exotic $\mathbb{R}^4$ property; unit radius n-ball attains maximum volume for $n = 5$ and maximum surface for $n = 7$, unit diameter n-ball attains maximum volume for $n = \{0, 1\}$ and maximum surface for $n = \{2, 3\}$, and so on.

But dimensionality of the graph of nature is by no means restricted to natural numbers. Negative and fractal (real) dimensions can be successfully applied in the fields of diffusion-limited aggregation and turbulence [9] for example. Perhaps negative dimensionalities define the realm of indistinguishable entities: bosons, fermions and anyons (the latter observable only in 2-dimensional systems), while positive dimensionalities define the realm of distinguishable ones [7]. A few arguments to support these claims are presented below.

Positive dimensions correspond to volumes, negative ones to densities [10].

Every simplicial n-manifold inherits a natural topology from $\mathbb{R}^n$ [11] and by researching Euclidean space $\mathbb{R}^n$ as a simplicial n-manifold topological (metric-independent) and geometrical (metric-dependent) content of the modeled quantities are disentangled [11]. This disentanglement is perhaps the most important virtue of the simplicial formulation. Yet it applies solely to natural dimensions. There are no n-simplices in negative [12] and fractal dimensions. The smallest dimensional simplex is (-1)-simplex (the void) which is degenerate (has undefined surface). Lack of simplices in negative dimensions implies that dissipative structures cannot be formed there. Only 2-simplices (triangles) enable a Delaunay flip allowing formation of dissipative structures (cf. Sections 5-7).

Also in negative, even dimensions n-balls have zero (void-like) volumes and zero (point-like) surfaces [13].

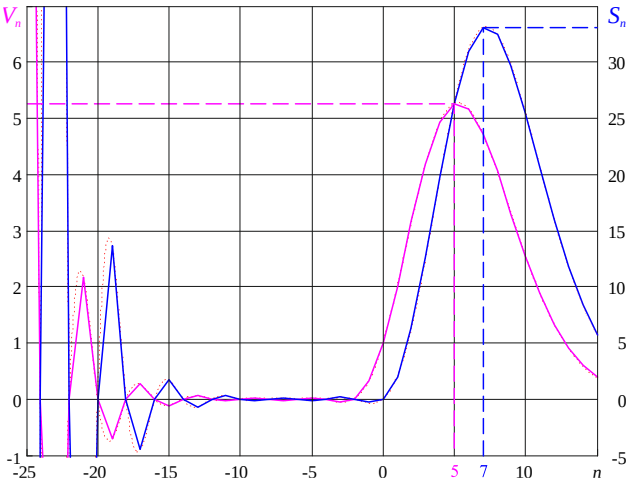

Fig. 1: Graphs of volumes (V) and surface areas (S) of n-balls of radius 1 for $n = -25, -6, \ldots, 15$.

There are countably infinitely many spherical harmonics but nature uses only the first four as subshells of s, p, d, and f electron shells that can hold 2, 6, 10, and 14 electrons respectively. Further subshells are not populated in ground states of all the observed elements. The first element that would require a g subshell (18 electrons) would have an atomic number of 121, while the heaviest element synthesized is Oganesson, with an atomic number of 118 and a half-life of about 1/1000 of a second.

Perhaps this is linked with properties of the unit radius n-balls in negative dimensions as illustrated in Fig. 1. The "flattening" occurring between dimensions -14 and -2 is intriguing. Dimensions -2, -6, -10, and -14 are bounded from both sides, with -14, that would represent the f subshell, already at the onset of divergence. In nature, the f subshell occurs essentially only in lanthanides and actinides.

3. Discretizations

The following discretizations are adopted in this paper. All masses M are w.l.o.g. taken as real multiplicities of the Planck mass m_P

$$M \doteq m\, m_P \quad m \in \mathbb{R}, \tag{2}$$

all lengths are w.l.o.g. taken as real multiplicities of the Planck length ℓ_P. However wavelengths are taken to be

$$\lambda \doteq l\, \ell_P \quad l \in \mathbb{R} \Big/ \{(-1,1)\}. \tag{3}$$

since a wavelength measures a 2π cycle and the minimum length of the cycle must be at least the Planck length, as no physical models describe smaller lengths. Thus the open set (-1, 1) is forbidden. With (2) and (3) one easily finds a relation between wavelength l and mass multiplier m in terms of the Compton wavelength

$$\lambda \doteq l\, \ell_P = \frac{h}{cm\, m_P} \quad \Leftrightarrow \quad l = \frac{2\pi}{m}. \tag{4}$$

Constraining to $l \geq 1$ yields

$$m \leq 2\pi, \tag{5}$$

which can be called the *threshold of distinguishability*, as it shows that particles having mases larger than $2\pi m_P$ have their Compton wavelengths smaller than the Planck length which is physically impossible. Such particles no longer feature wave-particle duality and they would not interfere with each other in the double-slit experiment; in principle they are always distinguishable.

Sphericality is, in general, considered in terms of diameter D, rather than radius R, and taken w.l.o.g. as

$$D \doteq d\, \ell_P \quad d \in \mathbb{R}. \tag{6}$$

Possible meaning of negative masses, wavelengths, and diameters is hinted further in Sections 9 and 10 and in Appendices. Complex wavelength multipliers l in (3) are briefly discussed in Section 9 but in general they are presently beyond the scope of this paper.

4. Discrete Black Holes

W.l.o.g. by expressing black hole mass using (2) and diameter using (6) the Schwarzschild diameter becomes

$$D_{BH} = \frac{4Gmm_P}{c^2} = \frac{4mG}{c^2}\sqrt{\frac{\hbar c}{G}} = 4m\ell_P = d\,\ell_P. \tag{7}$$

yielding a simple relation between black hole mass and diameter multipliers: $m = d/4$.

Thus the black hole *threshold of distinguishability* (5) in terms of a black hole diameter multiplier becomes

Preprints (www.preprints.org) | NOT PEER-REVIEWED | Posted: 25 November 2021 doi:10.20944/preprints202109.0368.v2

$$d \le 8\pi\,. \tag{8}$$

In other words only black holes having diameter multipliers below this bound have masses providing the Compton wavelength multiplier (4) larger than the Planck length. We shall return to it in Section 10.

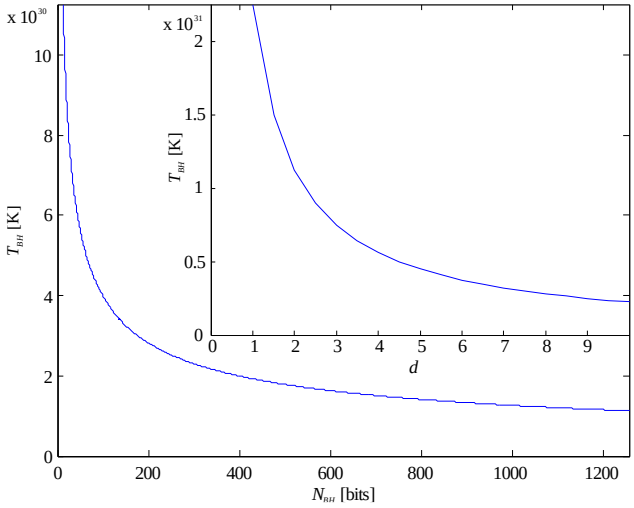

Fig. 2: Black hole temperature T_{BH} as a function of its informational capacity N_{BH} and diameter multiplier d.

According to the holographic principle [14, 15] bounded interior is separated from unbounded exterior by a 2-dimensional, spatial boundary. Having an area A, the boundary has an informational capacity $N_A = A/\ell_P^2 \in \mathbb{R}$ with one bit represented on the boundary by one Planck area ℓ_P^2. Therefore the number of bits the boundary provides is $\lfloor N_A \rfloor \in \mathbb{N}_0$. Black hole event horizon is a fundamental holographic boundary having only one geometric side observable as a 2-sphere. Using (6) the informational capacity of the event horizon is $N_{BH} = \pi D^2/\ell_P^2 = \pi d^2$. Plugging black hole surface gravity into Hawking radiation formula one arrives at the Hawking radiation temperature as a function of N_{BH} or diameter multipliers d

$$T_{BH} = \frac{m_P c^2}{2k_B\sqrt{\pi N_{BH}}} = \frac{T_P}{2\sqrt{\pi N_{BH}}} = \frac{T_P}{2\pi d}\,, \tag{9}$$

as illustrated in Fig. 2, where T_P denotes Planck temperature (cf. Appendices).

Since no physical models describe temperatures greater than the Planck temperature, the primordial Big Bang singularity temperature corresponds to black hole having $d = 1/(2\pi)$, $N_{BH} = 1/(4\pi)$ and $\lfloor N_{BH} \rfloor = 0$. At $d = 1$ black hole has temperature $T = T_P/2\pi$, which can be regarded as a reduced Planck temperature similarly as the reduced Planck constant or a reduced wavelength.

Natural multipliers d of black hole diameter are related to 2π cycle: black hole temperature (9) decreases by 2π factor with every integer increment of d.

Table 1 is a list of a few quantum black holes showing informational capacity, number of bits, gravitational potential with phasor θ set to 1 [8]

$$\delta\varphi = -\frac{4\pi c^2}{N_{BH}}\frac{\delta r}{\lambda\!\!\!^{-}} = -\frac{4\pi c^2}{N_{BH}}\theta\,, \tag{10}$$

mass and temperature of each hole as a function of its diameter multiplier d.

Diameter multiplier $d = 2\sqrt{2} \approx 2.83$ provides gravitational potential (10) equal to $-c^2/2$ and the mass of $d = 4$ black hole corresponds to Planck mass m_P [8]. Any *real* black hole such as Sagittarius A* ($M_{BH} \approx 8.62\text{e}36$ kg, $d \approx 1.58\text{e}45$, $N_{BH} \approx 7.88\text{e}90$) does not exist as an object in spacetime but is only observable as 2-sphere by observers that can only exist in $3 + i$ dimensions [5].

Table 1: Quantum black holes and dimensionality of the graph of nature

$d = D/\ell_P$	$N_{BH} = \pi d^2$	$\lfloor \pi d^2 \rfloor$	$\delta\varphi/c^2 = -4/d^2$	$M_{BH}/m_P = d/4$	$T_{BH}/T_P = 1/(2\pi d)$	black hole type/comments
$1/(2\pi)$	0.0796	0	$-16\pi^2$	0.0398	1	Big Bang (Planck temperature)
$1/\sqrt{\pi}$	1	1	-4π	0.1410	0.2821	min 1-bit, MB stat. singularity
$\sqrt{(\ln(4)/\pi)}$	1.3863	1	-9.0647	0.1661	0.2396	Landauer BH ($M_{BH}c^2 = Tk_B\ln(2)$)
$\sqrt{(2/\pi)}$	2	2	-2π	0.1995	0.1995	min 2-bit, FD stat. singularity
$\sqrt{(3/\pi)}$	3	3	-4.1888	0.2443	0.1629	min 3-bit
1	π	3	-4	0.25	0.1592	π-bit
$\sqrt{(4/\pi)}$	4	4	$-\pi$	0.2821	0.1410	min 4-bit, one unit of entropy
2	4π	12	-1	0.5	0.0796	12-bit
$2\sqrt{2}$	8π	25	-0.5	$1/\sqrt{2}$	0.0563	potential equal to $-GM/R_{BH} = -c^2/2$
3	9π	28	-0.4(4)	0.75	0.0531	28-bit
4	16π	50	-0.25	1	0.0398	$M_{BH} = m_P$
5	25π	78	-0.16	1.25	0.0318	
8π	$64\pi^3$	1984	-0.0063	2π	0.0063	$M_{BH} = 2\pi m_P$ ($\delta\varphi/c^2 + T_{BH}/T_P = 0$)

The number of bits on a black hole horizon is a natural number (OEIS A066643), while the black hole informational capacity (πd^2) is a transcendental number. Perhaps nature knows how to distinguish a set of vertices of a given black hole from a set of vertices of another one using the fractional part Fourier series expansion [16].

$$\{N_{BH}\} = \{\pi d^2\} = \frac{1}{2} - \frac{1}{\pi}\sum_{k=1}^{\infty}\frac{\sin\left(2k\pi^2 d^2\right)}{k}\,. \tag{11}$$

5. Delaunay Triangulated 2-Boundaries

Only Delaunay triangulation of a fixed point set V of vertices in $\mathbb{R}^n$ minimizes the Dirichlet energy [17]

Preprints (www.preprints.org) | NOT PEER-REVIEWED | Posted: 25 November 2021 doi:10.20944/preprints202109.0368.v2

$$E_D[\varphi] \doteq \frac{1}{2}\varphi^T L\varphi \tag{12}$$

of any piecewise linear function φ: $V \to \mathbb{R}$ over this point set (Rippa's theorem [18]), where L is the discrete cotan Laplacian. This is equal to say that the spectrum of the cotan Laplacian obtains its minimum on a Delaunay triangulation in the sense that the i-th eigenvalue of the cotan Laplacian of any other triangulation is bounded below by the i-th eigenvalue of the cotan Laplacian of the Delaunay triangulation [19].

A set of $n + 2$ points in n-space may be triangulated in at most 2 different ways and the *sphere test* selects a preferred one (Delaunay) of these two triangulations [20]. Yet in dimension three (or higher), there are nontriangulable non-convex polytopes [21]. Furthermore only Delaunay triangulation of a piecewise flat surface guarantees that edge weights of the cotan Laplacian are positive [22].

At least due to these two properties only 2-dimensional Delaunay triangulations are used by nature to create equipotential surfaces as holographic boundaries, where each triangle has at most one Planck area ℓ_P^2 representing 1 bit of rational information. Delaunay triangulated $\mathbb{R}^2$ boundary is equivalent to its continuous counterpart [11] and φ in (12) represents a harmonic potential assigned to vertices of the triangulation.

Any triangle on the boundary is a geodesic, non-planar one. A surface made of planar and geodesic triangles might not be twice differentiable as required by Laplace and Poisson's equations. Only Delaunay circles make the boundary "piecewise flat". Perhaps all boundaries are topological spheres and differ only with radii and uniqueness or the rank of non-uniqueness (i.e. the number of cyclic spherical quadrilaterals) of the triangulation.

Expressing the variation of entropy δS on an equipotential 2-dimensional surface A [23, eq. (1)[2]] (which is equivalent to the holographic boundary)

$$\delta S = -\frac{ck_B}{2G\hbar}\delta\varphi A, \tag{13}$$

where $\delta\varphi$ represents a variation of the potential on the boundary, as a function of the boundary informational capacity we arrive at

$$\delta S = -\frac{ck_B}{2G\hbar}\delta\varphi N_A \ell_P^2 = -\frac{1}{2}k_B N_A \frac{\delta\varphi}{c^2}. \tag{14}$$

This equation can be simplified by postulating a binary variation of the potential (or simply a binary potential) in Planck time t_P over k-th Planck triangle ℓ_P^2 defined as

$$\delta\varphi_k \doteq -\{0,1\}\,\ell_P^2/t_P^2 = -\{0,1\}\,c^2, \tag{15}$$

so that

$$\delta S = -\frac{1}{2}k_B \sum_{k=1}^{\lfloor N_A \rfloor} \frac{\delta\varphi_k}{c^2} = \frac{1}{2}k_B N_1, \tag{16}$$

where the summation goes over all Planck triangles of the boundary A, $N_1 \in \mathbb{N}$ denotes the number of Planck triangles that encode[3] $-c^2$, and triangle(s) of the fractional part $\{N_A\}$ of the boundary informational capacity encode(s) zero [8].

In this setting one Planck triangle that encodes $-c^2$ can be taken to represent one degree of freedom, so that the equipartition theorem

$$E = T\delta S = \frac{1}{2}k_B T \tag{17}$$

is recovered.

One vertex may be shared by many triangles, two vertices by two triangles. Only all three vertices of a triangle having the same potential of $-c^2/2$ provide unique association of $-c^2$ to this triangle. Therefore "active" vertex has gravitational potential of $-c^2/2$; "inactive" vertex has gravitational potential higher than $-c^2/2$ (diameter fluctuates, due to black hole absorption and emission). Planck triangle is "active" if all its vertices are active and then has gravitational potential of $-c^2$; otherwise it is "inactive" and encodes zero. Fractional part triangle(s) always encode(s) zero and its/their total area is lower than Planck area.

6. Delaunay Triangulated Black Hole Horizons

As an equipotential surface, black hole event horizon is also Delaunay triangulated.

Vertices define inner black hole polyhedrons that in turn define black hole cotan Laplacians and have area smaller than the area of the circumscribed sphere. The ratio of these areas rapidly converges toward unity as the size of the black hole increases.

It turns out that the temporary distribution of active triangles on an event horizon of a black hole tends to maximize Shannon entropy [8]. This results from comparing the entropic works on the event horizon with Hawking temperature and Bekenstein-Hawking entropy or the variation of binary entropy (16)

$$\begin{aligned}
T &= -\frac{\hbar}{2\pi c k_B}\nabla_R \phi_g \\
T\delta S &= \left(-\frac{\hbar}{2\pi c k_B}\frac{GM}{\frac{N_{BH}\ell_P^2}{4\pi}}\right)\left(\frac{1}{4}k_B N_{BH}\right) = -\frac{1}{2}Mc^2 \\
T\delta S &= \left(-\frac{\hbar}{2\pi c k_B}\frac{GM}{\frac{N_{BH}\ell_P^2}{4\pi}}\right)\left(\frac{1}{2}k_B N_1\right) = -\frac{N_1}{N_{BH}}Mc^2 \\
-\frac{1}{2}Mc^2 &= -\frac{N_1}{N_{BH}}Mc^2 \Leftrightarrow N_1 = \frac{1}{2}N_{BH}
\end{aligned} \tag{18}$$

In other words, the event horizon is a truly random binary message containing a balanced number of Planck

[2] The additive constant in this equation may be taken to represent the fractional part $\{N_A\}$ of the holographic boundary informational capacity.

[3] Binary potential was originally defined as a positive quantity. This is, however, in conflict with the negative value of the gravitational potential at a vertex of the event horizon ($-c^2/2$). Also $(ic/\sqrt{2})^2 = -c^2/2$. Variation of the potential requires the notion of time and time is imaginary.

Preprints (www.preprints.org) | NOT PEER-REVIEWED | Posted: 25 November 2021 doi:10.20944/preprints202109.0368.v2

area triangles encoding binary potential (15) equal to $-c^2$ and 0. At $d = 2\sqrt{2}$ black hole provides gravitational potential (10) equal to $-c^2/2$ at each vertex; but such a black hole is static, as all its Planck triangles are active. Only larger black holes such as 9π-bit black hole ($d = 3$) can at certain vertices have potential (10) larger than $-c^2/2$ and thus are capable of generating a truly random message.

Another simple observation is that the average potential on the event horizon equals the event horizon potential at a vertex; that is

$$\frac{\sum_{k=1}^{N_1}\left(-c^2\right)+\sum_{k=1}^{\lfloor N_{BH}\rfloor-N_1}0}{N_{BH}}=\frac{-N_1c^2}{N_{BH}}=\frac{-\frac{1}{2}N_{BH}c^2}{N_{BH}}=-\frac{1}{2}c^2 . \quad (19)$$

N_{BH}-bit black hole provide $2^{\lfloor N_{BH}\rfloor}$ arrangements of Planck triangles. These arrangements can thus represent a set of addresses a_m of vertices $m = 1, 2,\ldots, 2^{\lfloor N_{BH}\rfloor}$ of a unit n-cube (in units of $-c^2$) ordered in certain way (binary, Gray code, etc.). Then the following holds

$$\frac{-\sum_{m=1}^{2^{\lfloor N_{BH}\rfloor}}a_m(i)c^2}{2^{\lfloor N_{BH}\rfloor}}=-\frac{1}{2}c^2, \quad (20)$$

where $i = 1, 2,\ldots, \lfloor N_{BH}\rfloor$ is n-cube coordinate. In other words the quotient of the sum of each triangle activations within the set of all triangle arrangements to the cardinality of this set equals the event horizon potential at a vertex. The meaning of this relation remains to be researched.

To generate a truly random message (18) a black hole event horizon must have uniquely defined Delaunay triangulation with at least one spherical triangle having an area corresponding to the fractional part of its informational capacity $\{N_{BH}\} = N_{BH} - \lfloor N_{BH}\rfloor$, and all the remaining triangles having Planck areas. Uniquely defined means that no four vertices on the event horizon share a common circle [24], which is equal to say that no two triangles on the event horizon form a cyclic spherical quadrilateral. Two regular (uniquely defined) Delaunay triangles have $N_{BH} = 2$ (and two circumcenters), but two equally possible orientations of a diagonal on a cyclic spherical quadrilateral (in particular on a spherical rectangle) having vertices, say 1 to 4, and only one circumcenter would enable to assign an additional bit to this pair of triangles. Certainly triangles {1,2,3} and {1,3,4} are different than triangles {1,2,4} and {2,3,4} even if in both cases they would encode $-c^2$. Thus, non-uniquely defined Delaunay triangulation of a black hole event horizon would simply invalidate the Bekenstein bound on black hole entropy [14].

Therefore a black hole is a fundamental, one-sided limit of thermodynamic equilibrium for all the remaining dissipative structures of nature in. It emits informationless, diameter dependent (9) blackbody radiation characterized by zero Gibbs free energy and representing the degenerate case of relativistic Bose-Einstein statistics (32) [25]. Informationless nature of blackbody radiation is further asserted by the no-hiding theorem [26].

7. Delaunay Triangulated Boundaries of Two-Sided Dissipative structures

A two-sided dissipative structure operates out of thermodynamic equilibrium and thus do not generate a truly random message (18). I is enclosed by non-uniquely defined Delaunay triangulated boundary. This allows it to use the additional bits provided by cyclic geodesic quadrilaterals (enabling Delaunay flips) to locally decrease entropy, staying away of thermodynamic equilibrium. Obviously such quadrilaterals are scarce in the graph of nature but this is confirmed by scarceness of dissipative structures such as planets, stars (excluding neutron stars and white dwarfs), hurricanes, living organisms, etc. in observable nature.

Similarly to black holes, two-sided boundaries are also topological spheres and differ only with their informational capacity and the rank of non-uniqueness (i.e. the number of cyclic spherical quadrilaterals) of the triangulation. In particular stars are two-sided dissipative structures and their non-degenerate radiation and the departure from the informationless blackbody radiation [25] stems from the non-maximal Shannon entropy.

A relation between non-uniqueness of the triangulation for cyclic geodesic quadrilaterals and zero weights of the cotan Laplacian only for geodesic rectangles requires further research. Any one of the two possible triangulations on 4 vertices of a rectangle produces the same cotan Laplacian [5]. Yet there exist isospectral but non-isometric manifolds.

8. Black Hole Blackbody Radiation

Thus Planck's law for blackbody spectral radiance

$$B_\lambda(\lambda,T)=\frac{2hc^2}{\lambda^5}\frac{1}{\exp\left(hc/\lambda k_BT\right)-1}, \quad (21)$$

plugging $\lambda := l\ell_P$ and black hole temperature (9) is

$$B_{BH}(l,d)=\frac{2hc^2}{l^5\ell_P^5}\frac{1}{\exp\left(4\pi^2d/l\right)-1} \quad (22)$$

for wavelength or

$$B_{BH}\left(\frac{c}{l\ell_P},d\right)=\frac{2hc}{l^3\ell_P^3}\frac{1}{\exp\left(4\pi^2d/l\right)-1} \quad (23)$$

for frequency.

Black hole blackbody spectral radiance is almost like a bump function with measurable EMR ($W\cdot sr^{-1}\cdot m^{-2}\cdot m^{-1}$) in a wavelength range of 10^{-12} to 10^{12} meter for a black hole of a size of an angstrom (d = 1e25). Radiance of smaller holes vanishes for larger wavelengths; radiance of bigger ones vanishes for smaller wavelengths. Relations (21)-(23) are, as such, spacetime dimensional (they are derived under the assumption of a 2-sphere emitting blackbody radiation).

9. Black Hole Diameter Fluctuations

Black hole absorption was studied by Jacob Bekenstein [14] to derive his famous bound on black hole entropy ($S_{BH} = k_BN_{BH}/4$). Emission was shown by Steven

Preprints (www.preprints.org) | NOT PEER-REVIEWED | Posted: 25 November 2021 doi:10.20944/preprints202109.0368.v2

Hawking [27] to be responsible for micro black holes collapses. Taking both processes together the black hole mass and thus also its diameter fluctuates in time.

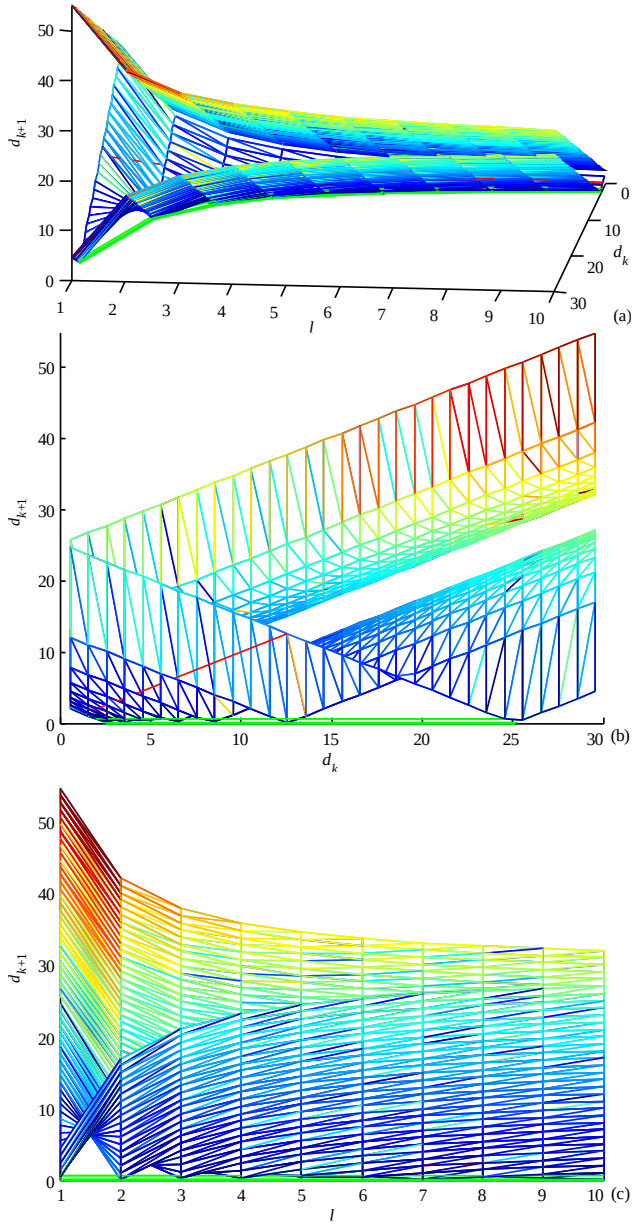

Fig. 3: New 2-sphere black hole diameter d_{k+1} after absorption (a-c) and emission (b, c) of a particle having wavelength l. Red curve represents constant diameter, three green ones - black hole collapse w/r/t $d_{k+1} = \{0, 1/(2\pi), 1/\sqrt{\pi}\}$. Sinusoidal characteristic of collapse is due to l drawn as a natural number.

Informationless black hole absorption [14, 28] and emission [8] formulas for a subatomic particle having a wavelength corresponding to the black hole radius can be extended (cf. Appendices) to arbitrary wavelengths l

$$N_{A/E}(d,l) = 64\pi^3 \frac{1}{l^2} \pm 16\pi^2 \frac{d}{l} + \pi d^2, \qquad (24)$$

which can be described more compactly ($N_{BH} = \pi d^2$) as a recurrence relation

$$d_{k+1}^{A/E} = \sqrt{64\pi^2 \frac{1}{l^2} \pm 16\pi \frac{d_k}{l} + d_k^2} \qquad (25)$$

describing new diameter d_{k+1} of a black hole (2-sphere) having an initial diameter d_k after absorbing (A, "+") or emitting (E, "-") a subatomic particle having a wavelength l, as illustrated in Fig. 3.

This derivation can be taken to other dimensions yielding the following recurrence relation for black hole ((n-1)-sphere[4]) diameter after absorption (A, "+") or emission (E, "-") of a wavelength l

$$\left(d_{k+1}^{A/E}\right)^{n-1} = \left(d_k \pm \frac{8\pi}{l}\right)^{n-1}. \qquad (26)$$

Note that equations (25) and (26) are time dependent. RHS represents initial state, while LHS final state of a black hole after absorption/emission of a wavelength l.

As one-sided thermodynamic equilibrium limit for a dissipative structure, black holes can certainly be studied also in (n + i)-dimensions. Otherwise all two-sided dissipative structures require (3 + i)-dimensional interiors bounded by (2 + i)-dimensional boundaries.

There are at least three distinct thresholds of a black hole collapse after emission of a wavelength l that can be derived from (26):

1. $d_{k+1}^E = 0$ total collapse;
2. $d_{k+1}^E = 1/(2\pi)$ Planck temperature collapse; and
3. $d_{k+1}^E = 1/\sqrt{\pi}$ one bit collapse.

Thus total black hole collapse occurs after emission of a particle having a wavelength $l = 8\pi/d_k$. For Sagittarius A* ($d_k \approx$ 1.58e45) l = 1.59e-44 << 1, so Sagittarius will never collapse.

If we now set $l \geq 1$ in (26) we arrive at

$$d_k \leq 8\pi \approx 25.132, \qquad (27)$$

for $d_{k+1}^E = 0$,

$$d_k \leq \frac{1+16\pi^2}{2\pi} \approx 25.292, \qquad (28)$$

for $d_{k+1}^E = 1/(2\pi)$, and

$$d_k \leq \frac{1+8\pi\sqrt{\pi}}{\sqrt{\pi}} \approx 25.697, \qquad (29)$$

for $d_{k+1}^E = 1/\sqrt{\pi}$; the bounds for a maximum diameters of collapsible black holes. The lowest bound $d_k \leq 8\pi$ corresponds to a black hole having mass 2π times greater than the Planck mass or lower. We have already derived this bound as (8), while considering admissible black hole Compton wavelength.

Black hole diameter does not change ($d_{k+1}^E = d_k$) after emission of wavelengths listed in Table 2. Relation (26) is symmetrical w/r/t n = 1, i.e. the wavelengths solving $d_{k+1}^E = d_k$ are the same for n and 2 - n. This is a reflection relation around 2.

Analytical formula $l(n)$ for constant diameter emission in any dimension, if one exists, remains to be researched. Odd dimensionalities admit real wavelength $l = 4\pi/d_k$. In even dimensionalities all constant diameter wavelengths in Table 2 are complex, which hints an existence of a link

[4] the term n-ball is a misnomer for a black hole, as it suggests that the black hole has an interior.

Preprints (www.preprints.org) | NOT PEER-REVIEWED | Posted: 25 November 2021 doi:10.20944/preprints202109.0368.v2

with vanishing volumes and vanishing surfaces of *n*-balls in negative, even dimensions. Surfaces of *n*-cubes inscribed in such exotic *n*-balls are imaginary [13].

Table 2: Emission wavelength l that keeps black hole diameter constant in integer dimensions n = -7, -6,…,9.

n	l maintaining constant black hole diameter
-7, 9	$l_1=\frac{4\pi}{d_k}, l_{2,3,4,5}=\frac{4\pi}{d_k}\left(1\pm i\sqrt{3\pm 2\sqrt{2}}\right)$ $l_{6,7}=\frac{4\pi}{d_k}(1\pm i)$
-6, 8	complicated and complex solution
-5, 7	$l_1=\frac{4\pi}{d_k}, l_{2,3}=\frac{4\pi}{d_k}\left(1\pm\sqrt{3}i\right), l_{4,5}=\frac{4\pi}{d_k}\left(1\pm\frac{\sqrt{3}}{3}i\right)$
-4, 6	$l_{1,2,3,4}=\frac{4\pi}{d_k}\left(1\pm\frac{\sqrt{5\pm 2\sqrt{5}}}{\sqrt{5}}i\right)$
-3, 5	$l_1=\frac{4\pi}{d_k}, l_{2,3}=\frac{4\pi}{d_k}(1\pm i)$
-2, 4	$l_{1,2}=\frac{4\pi}{d_k}\left(1\pm\frac{\sqrt{3}}{3}i\right)$
-1, 3	$l=4\pi/d_k$
0, 2	contradiction ($1\neq 0$)
1	identity ($1=1$)

Informational capacity (24) of a black hole observable as a 2-sphere after absorption of a wavelength l can be transformed to

$$\pi\frac{d_{k+1}^2}{d_k^2}=64\pi^3\frac{1}{d_k^2l^2}+16\pi^2\frac{1}{d_kl}+\pi, \tag{30}$$

where d_k is the black hole diameter before and d_{k+1} after absorption. This has the same algebraic form as the algebraic definition [29] of the inverse of the fine structure constant

$$\alpha^{-1}\doteq 4\pi^3+\pi^2+\pi\approx 137.036 \tag{31}$$

Both these formulas are apparently related but this relation remains to be researched.

10. Black Holes Quantum Statistics

If a black hole Planck triangle emits/absorbs a photon (boson), as it changes its state from active to inactive or vice versa and an electron (fermion) energy level is respectively decreased/increased in this interaction, then the event horizon can be described by Bose-Einstein (BE) and Fermi-Dirac (FD) statistics with degeneracy interpreted as the number of Planck triangles $\lfloor\pi d^2\rfloor$ on the event horizon. No Planck triangle is distinct and each one is equally capable of emitting/absorbing a subatomic particle having energy corresponding to wavelength multiplier l. There are certainly no dedicated microwave or X-ray triangles on the horizon. These spacetime dimensional (due to $\lfloor\pi d^2\rfloor$ term) statistics along with the Maxwell–Boltzmann[5] (MB) one are thus as follows

$$N_{BE}(d,l)=\frac{\lfloor\pi d^2\rfloor}{e^{4\pi^2d/l}-1}, \tag{32}$$

$$N_{MB}(d,l)=\frac{\lfloor\pi d^2\rfloor}{e^{4\pi^2d/l}}, \tag{33}$$

$$N_{FD}(d,l)=\frac{\lfloor\pi d^2\rfloor}{e^{4\pi^2d/l}+1}, \tag{34}$$

as illustrated in Fig. 4, where $N(d, l)$ is the average number of bosons, classical particles, and fermions, respectively, having wavelength l.

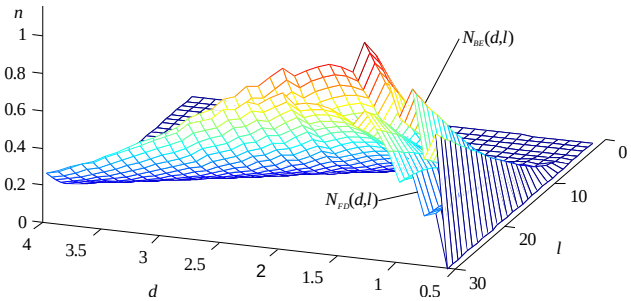

Fig. 4: Bose-Einstein (BE, top) and Fermi-Dirac (FD, bottom) 2-sphere black hole statistics.

The nontrivial black hole microstate degeneracy starts at 3 vertices [30] of the Voronoi triangulation that corresponds to the π-bit black hole with 4 vertices.

For $N>0$ photons to be emitted/absorbed or $N>0$ electron energy levels to be respectively decreased/increased on average, $N(d,l)\geq N$ and the following bounds, illustrated in Fig. 5 for $N=1$, are obtained from statistics (32)-(34)[6]

$$l_{BE}(d,N)\geq\frac{4\pi^2d}{\ln\left(\pi d^2+N\right)-\ln(N)}, \tag{35}$$

$$l_{MB}(d,N)\geq\frac{4\pi^2d}{\ln\left(\pi d^2\right)-\ln(N)}, \tag{36}$$

$$l_{FD}(d,N)\geq\frac{4\pi^2d}{\ln\left(\pi d^2-N\right)-\ln(N)}, \tag{37}$$

Each bound has the singularity

$$d_{BE}^{\sin}=0,\ d_{MB}^{\sin}=\pm\sqrt{\frac{N}{\pi}},\ d_{FD}^{\sin}=\pm\sqrt{\frac{2N}{\pi}}, \tag{38}$$

and minimum

$$d_{BE}^{\min}=\pm\sqrt{-N\left(\frac{W_0\left(-2e^{-2}\right)+2}{\pi W_0\left(-2e^{-2}\right)}\right)},\ d_{MB}^{\min}=\pm e\sqrt{\frac{N}{\pi}},\ d_{FD}^{\min}=\pm\sqrt{N\frac{W_0\left(2e^{-2}\right)+2}{\pi W_0\left(2e^{-2}\right)}} \tag{39}$$

where $W_0(x)$ is the Lambert W function (the omega function). Minima are listed in Table 3 along with corresponding minimum wavelengths.

Negative wavelengths for positive diameters can be interpreted in terms of emission/absorption, with positive wavelengths representing black hole absorption and nega-

[5] MB statistics lies between BE and FD statistics.

[6] $n\leq\lfloor x\rfloor\leftrightarrow n\leq x$ (property of the floor function).

Preprints (www.preprints.org) | NOT PEER-REVIEWED | Posted: 25 November 2021 doi:10.20944/preprints202109.0368.v2

tive wavelengths representing black hole emission. BE bound (35), having no negative wavelengths, illustrates that bosons (photons) cannot escape from a black hole.

Table 3: BE, MB, and FD bounds for N = 1, 2,…,6.

N	d^{min}_{BE}	l^{min}_{BE}	d^{min}_{MB}	l^{min}_{MB}	d^{min}_{FD}	l^{min}_{FD}
1	1.1173	27.678	1.5336	30.273	1.8007	32.054
2	1.5800	39.142	2.1689	42.812	2.5465	45.332
3	1.9352	47.939	2.6563	52.434	3.1188	55.520
4	2.2345	55.355	3.0673	60.545	3.6013	64.109
5	2.4982	61.889	3.4293	67.692	4.0264	71.676
6	2.7367	67.796	3.7566	74.152	4.4107	78.517

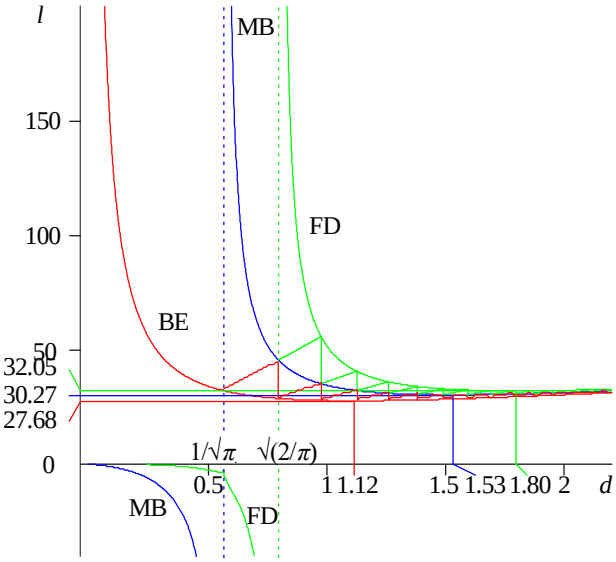

Fig. 5: Wavelength bounds for BE (red), MB (blue), and FD (green) statistics for Delaunay triangulated black hole as a function of diameter/dimensionality d with N = 1.

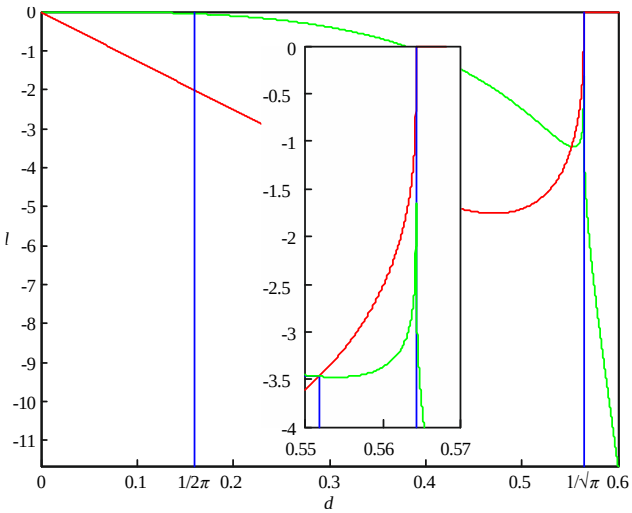

Fig. 6: Real (green) and imaginary (red) part of the wavelength bound for FD statistics as a function of d in the vicinity of $1/\sqrt{\pi}$.

For $0 < d \leq \sqrt{(N/\pi)}$ wavelengths l given by FD bound (37) are complex, as shown in Fig. 6. Below this threshold, which corresponds to the diameter of 1-bit black hole, black hole emits complex wavelengths and only after exceeding this diameter they become *real* and thus observable. Perhaps only negative and real wavelengths in the FD bound (37) within the range $\sqrt{(N/\pi)} < d \leq \sqrt{(2N/\pi)}$ represent Hawking radiation of fermions. Interestingly the real part of the wavelength below $d = 1/(2\pi)$ Planck temperature threshold vanishes.

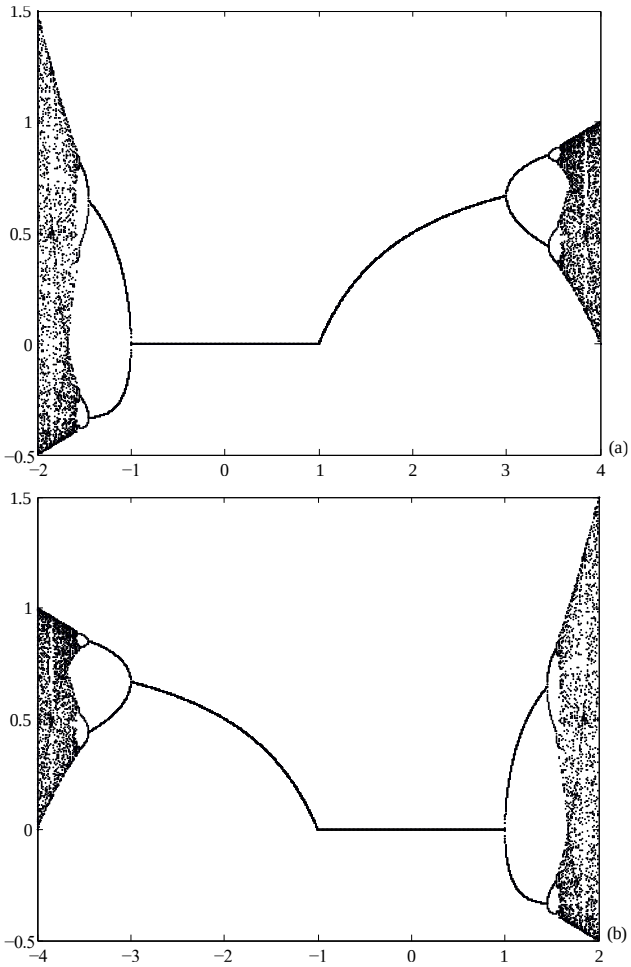

Fig. 7: Bifurcation diagrams of the logistic maps corresponding to FD (a) and BE (b) statistics along with attractor boundaries.

The logistic function

$$f_{FD}(d) = \frac{1}{e^{-\mu d}+1} = \frac{e^{\mu d}}{e^{\mu d}+1}, \tag{40}$$

where μ determines its steepness has derivative

$$f'_{FD}(d) = \mu f_{FD}(d)\left[1 - f_{FD}(d)\right] = \frac{\mu}{4\cosh^2(\mu d/2)}, \tag{41}$$

which is the continuous version of the logistic map

$$x^{FD}_{n+1} = \mu x^{FD}_n \left(1 - x^{FD}_n\right), \tag{42}$$

having a bifurcation diagram shown in Fig. 7(a). For certain values of μ within the range of $-2 \leq \mu \leq 4$ [31] (for $\mu < -2$ and $\mu > 4$ (42) is divergent), in particular for $-2 \leq \mu \leq -1$ and $3 \leq \mu \leq 4$, the logistic map displays intermittent (irregular alternation of periodic and chaotic dynamics) behavior.

A similarity of the logistic function and FD statistics is apparent (hence the index *FD*). Comparing FD statistics (34) with the logistic function (40) we conclude that

$$\mu = \frac{4\pi^2}{l}, \tag{43}$$

with $\max(\mu) = 4\pi^2 \approx 39.4784$ (for l = 1) and

Preprints (www.preprints.org) | NOT PEER-REVIEWED | Posted: 25 November 2021 doi:10.20944/preprints202109.0368.v2

$$e^{\mu d} = \lfloor \pi d^2 \rfloor. \tag{44}$$

Plugging (43) to (44) and solving for l leads to

$$l_{FD}(d) = \frac{4\pi^2 d}{\ln\left(\lfloor \pi d^2 \rfloor\right)}, \tag{45}$$

the equation resembling wavelength bound for MB statistics (36). A similar relation

$$l_{BE}(d) = \frac{4\pi^2 d}{\ln\left(\lfloor \pi d^2 \rfloor + 1\right)} \tag{46}$$

can by postulated for wavelength bound for BE statistics (35). This leads to the BE logistic function

$$f_{BE}(d) = \frac{1}{1 - e^{-\mu d}} = \frac{e^{\mu d}}{e^{\mu d} - 1} \tag{47}$$

having derivative

$$f'_{BE}(d) = \mu f_{BE}(d)\left[f_{BE}(d) - 1\right] = \frac{-\mu}{4\sinh^2(\mu d/2)}, \tag{48}$$

which is the continuous version of the BE logistic map

$$x_{n+1}^{BE} = \mu x_n^{BE}\left(x_n^{BE} - 1\right) \tag{49}$$

having a bifurcation diagram shown in Fig. 7(b). It displays intermittent behavior for $-4 \le \mu \le -3$ and $1 \le \mu \le 2$ and is divergent for $\mu < -4$ and $\mu > 2$. Obviously (42) turns into (49) by swapping μ with $-\mu$. Negative μ by virtue of (43) corresponds to negative wavelengths.

Relations (45) and (46) illustrated in Fig. 5 have form of a sawtooth waves. For $N = 1$ the BE wave (46) bounces between the BE wavelength bound (35) and the MB wavelength bound (36), while the FD wave (45) bounces between the MB wavelength bound (36) and the FD wavelength bound (37).

Checking intermittent values of the parameter μ in maps (42) and (49) in dependence of l given by (43) yields

$$3 \le \mu \le 4 \quad \Leftrightarrow \quad \pi^2 \le l \le \frac{4}{3}\pi^2 \tag{50}$$

for the FD logistic map (42) (with no common part for $-2 \le \mu \le -1$) and

$$1 \le \mu \le 2 \quad \Leftrightarrow \quad 2\pi^2 \le l \le 4\pi^2 \tag{51}$$

for the BE logistic map (49) (with no common part for $-4 \le \mu \le -3$).

Convergence bounds of the maps (42) and (49) are related: $(-2)^2 = 4$ and $(2i)^2 = -4$. On the other hand the logistic function (40) has codomain $0 < f_{FD} < 1$, while the BE logistic function (47) has codomain $-\infty < f_{BE} < 0$ and $1 < f_{BE} < \infty$, which renders range $(0, 1)$ distinct to the range $(-1, 0)$. A similar asymmetry has been observed for graphene [32] with regard to the positive and negative number of layers.

Black hole interaction with the environment described in this way certainly requires further research taking into account the imaginary set of Planck units [33].

11. Discussion

An improved model of a black hole interaction with the environment remains to be researched. It might provide further insight into the sonoluminescence phenomenon, the mechanism of which remains unknown.

Blackbody radiation carries no information and depends only on temperature of a radiating object. This informationless feature relates blackbody radiation with a truly random message of $\{0, -c^2\}$ (18). For black holes blackbody radiation spectrum is determined solely by its informational capacity (diameter) (9). This size dependence is uneasy. Fortunately black holes are not the only observable objects that emit blackbody radiation. Neutron stars supported against collapse by neutron degeneracy pressure and white dwarfs supported by electron degeneracy pressure, both pressures due to the Pauli exclusion principle, also emit blackbody radiation. Thus they also have unique Delaunay triangulations, generate truly random messages (a thermodynamic equilibrium blackbody radiation), and also invalidate the Jordan-Brouwer separation theorem, the generalized Stokes theorem, and the no-hiding theorem [26].

Interiors of living cells were exploited by biological evolution, beginning with coacervates. An open question is why would a hurricane need an interior?

Acknowledgments

I thank Mirek, who found that black holes invalidate Jordan-Brouwer separation theorem, for helpful discussions and encouragement.

[1] Ludwig Boltzmann, “Über die Beziehung zwischen dem zweiten Hauptsatze des mechanischen Wärmetheorie und der Wahrscheinlichkeitsrechnung, respective den Sätzen über das Wärmegleichgewicht” Von dem c. M. Ludwig Boltzmann in Graz Sitzb. d. Kaiserlichen Akademie der Wissenschaften, mathematich-naturwissen Cl. LXXVI, Abt II, 1877, pp. 373-435., av. at http://users.polytech.unice.fr/~leroux/boltztrad.pdf.

[2] Thomas S. Kuhn, “Black-Body Theory and the Quantum Discontinuity, 1894-1912”. Oxford University Press, 1978.

[3] Pierre Teilhard de Chardin, “The Phenomenon of Man”. Paris, Éditions du Seuil. 1955.

[4] John Archibald Wheeler, “Proc. 3rd Int. Symp. on Foundations of Quantum Mechanics". p.354 (Phys. Soc. Japan (1990), Tokyo, 1989).

[5] Szymon Łukaszyk, “Four Cubes”. arXiv:2007.03782 [math.GM], 7 Jul 2020.

[6] Rudolf Carnap, “The philosophy of Rudolf Carnap”. Open Court, 1963.

[7] Ilya Prigogine, Isabelle Stengers, “Order Out of Chaos: Man's New Dialogue with Nature”. Bantam Books, April 1984.

[8] Szymon Łukaszyk, “Black hole horizons as binary messages”. arXiv:1910.11081 [physics.gen-ph], 15 Feb 2021.

[9] Benoit B. Mandelbrot, “Negative Fractal Dimensions And Multifractals”. Physica A 163 (1990) 306-315.

[10] https://tglad.blogspot.com/2017/08/reframing-geometry-to-include-negative.html

[11] Mathieu Desbrun, Eva Kanso, Yiying Tong, “Discrete Differential Forms for Computational Modeling”. Discrete

Differential Geometry. Oberwolfach Seminars, vol 38. Birkhäuser Basel (2008).
[12] Szymon Łukaszyk, "New Recurrence Relation for Volumes of Regular n-Simplices in Integer Dimensions". DOI: 10.13140/RG.2.2.23828.83840, October 2021.
[13] Szymon Łukaszyk, "A simple recursive formula for volumes and surfaces of n-balls". DOI: 10.13140/RG.2.2.14751.38566, May 2020.
[14] J.D. Bekenstein, "Black holes and entropy". Phys. Rev. D 7 (1973) 2333 (http://www.scholarpedia.org/article/Bekenstein_bound, http://www.scholarpedia.org/article/Bekenstein-Hawking_entropy).
[15] Erik Verlinde, "On the Origin of Gravity and the Laws of Newton". Journal of High Energy Physics, doi:10.1007/JHEP04(2011)029, arXiv:1001.0785v1 [hep-th] 6 Jan 2010.
[16] Edward Charles Titchmarsh, David Rodney Heath-Brown, "The Theory of the Riemann Zeta-function (2nd ed.)". Oxford: Oxford U. P., ISBN 0-19-853369-1.
[17] Max Wardetzky, "Generalized Barycentric Coordinates in Computer Graphics and Computational Mechanics". Chapter 5, A Primer on Laplacians, CRC Press, 2017.
[18] Samuel. Rippa, "Minimal roughness property of the Delaunay triangulation". Comput. Aided Geom. Design 7, 489–497, 1990.
[19] Renjie Chen, Yin Xua, Craig Gotsman, Ligang Liu, "A spectral characterization of the Delaunay triangulation". Computer Aided Geometric De-sign, Elsevier Vol. 27, Issue 4, May 2010.
[20] Charles L. Lawson, "Properties of n-dimensional triangulations". Computer Aided Geometric Design 3 (1986) 231-246.
[21] Jesús A. De Loera, et al., "Triangulations, Structures for Algorithms and Applications". DOI 10.1007/978-3-642-12971-1, Springer 2010.
[22] Alexander I. Bobenko, Boris A. Springborn, "A Discrete Laplace–Beltrami Operator for Simplicial Surfaces". Discrete Comput Geom (2007) 38: 740–756.
[23] Sabine Hossenfelder, "Comments on and Comments on Comments on Verlinde's paper "On the Origin of Gravity and the Laws of Newton". arXiv:1003.1015v1 [gr-qc] 4 Mar 2010.
[24] Veronica G. Vergara Larrea, "Construction of Delaunay Triangulations on the Sphere: A Parallel Approach". Florida State University Libraries, Electronic Theses, Treatises and Dissertations, 2011.
[25] Kothari, D. S., and B. N. Singh, "Bose-Einstein Statistics and Degeneracy". Proceedings of the Royal Society of London. Series A, Mathematical and Physical Sciences, vol. 178, no. 973, 1941, pp. 135–152.
[26] Samuel L. Braunstein and Arun K. Pati, "Quantum Information Cannot Be Completely Hidden in Correlations: Implications for the Black-Hole Information Paradox". Phys. Rev. Lett. 98, 080502 –23 February 2007.
[27] Stephen Hawking, "Black hole explosions?". Nature. 248 (5443): 30–31. 1974 (http://www.scholarpedia.org/article/Hawking_radiation).
[28] Leonard Susskind, "Black Hole War: My Battle with Stephen Hawking to Make the World Safe for Quantum Mechanics". Little, Brown and Company, July 7, 2008.
[29] Péter Várlaki, László Nádai, József Bokor, "Number Archetypes and 'Background' Con-trol Theory Concerning the Fine Structure Constant". Acta Polytechnica Hungarica Vol. 5, No. 2, 2008.
[30] Aharon Davidson, "From Planck area to graph theory: Topologically distinct black hole microstates". Phys. Rev. D 100, 081502(R) – Published 18 October 2019.
[31] Tsuchiya, Takashi; Yamagishi, Daisuke, "The Complete Bifurcation Diagram for the Logistic Map". Z. Naturforsch. 52a: 513–516. 11 Feb 1997.
[32] Szymon Łukaszyk, "A short note about the geometry of graphene". DOI: 10.13140/RG.2.2.11500.18569, November 2020.
[33] Szymon Łukaszyk, "A short note about graphene and the fine structure constant". DOI: 10.13140/RG.2.2.21718.88641, October 2020.

Appendices

1. Derivation of black hole temperature (9):

$$T = \frac{T_P}{2\pi d} = \frac{T_P}{2\pi}\frac{\ell_P}{2R_{BH}} = \frac{T_P \ell_P}{4\pi}\frac{c^2}{2GM} = \\ = \frac{c^2}{8\pi GM}\sqrt{\frac{\hbar c^5}{Gk_B^2}}\sqrt{\frac{\hbar G}{c^3}} = \frac{\hbar c^3}{8\pi G k_B M} \tag{52}$$

2. Another form of Planck-Einstein relation:

$$E = h\nu = h\frac{c}{\lambda} = \frac{hc}{l\ell_P} = \frac{2\pi\hbar c}{l}\sqrt{\frac{c^3}{\hbar G}} = \\ = \frac{2\pi}{l}\frac{k_B}{k_B}\sqrt{\frac{\hbar^2 c^2 c^3}{\hbar G}} = \frac{2\pi}{l}k_B T_P \tag{53}$$

3. Derivation of black hole diameter fluctuations.

After absorbing/emitting a subatomic particle having a wavelength l 2-sphere black hole diameter defined by its mass increases(+)/decreases(-) by the Compton mass $m = h/(c\lambda)$ of this particle. Thus we arrive at

$$D^{A/E} = D \pm \delta D = d\ell_P \pm \frac{4G}{c^2}\frac{2\pi\hbar}{cl\ell_P} \\ = d\ell_P \pm \frac{8\pi\hbar G}{lc^3\ell_P} = d\ell_P \pm \frac{8\pi\ell_P}{l} = \left(d \pm 8\pi/l\right)\ell_P \tag{54}$$

Accordingly black hole area increases/decreases as well

$$A^{A/E} = \pi\left(d^{A/E}\right)^2\ell_P^2 = \pi\left(d\ell_P \pm \frac{8\pi G\hbar}{c^3 l\ell_P}\right)^2 \\ \pi\left(d^{A/E}\right)^2\ell_P^2 = \pi\left(d\ell_P \pm \frac{8\pi}{l}\ell_P\right)^2 = \\ = \pi\ell_P^2\left(d \pm \frac{8\pi}{l}\right)^2 \tag{55}$$

$$\left(d_{k+1}^{A/E}\right)^2\ell_P^2 = d_k^2\ell_P^2 \pm 2d_k\ell_P\frac{8\pi G\hbar}{c^3 l\ell_P} + \frac{64\pi^2 G^2\hbar^2}{c^6 l^2\ell_P^2} \\ \left(d_{k+1}^{A/E}\right)^2 = d_k^2 \pm \frac{16\pi d_k G\hbar}{c^3 l\ell_P^2} + \frac{64\pi^2 G^2\hbar^2}{c^6 l^2\ell_P^4} = \\ = d_k^2 \pm \frac{16\pi d_k G\hbar}{c^3 l}\frac{c^3}{\hbar G} + \frac{64\pi^2 G^2\hbar^2}{c^6 l^2}\frac{c^6}{\hbar^2 G^2} = \\ = d_k^2 \pm 16\pi\frac{d_k}{l} + 64\pi^2\frac{1}{l^2} \tag{56}$$

If $l = d/2$ [14, 28] then

Preprints (www.preprints.org) | NOT PEER-REVIEWED | Posted: 25 November 2021 doi:10.20944/preprints202109.0368.v2

$$d_{k+1}^{A/E} = \pm\sqrt{256\pi^2 \frac{1}{d_k^2} \pm 32\pi + d_k^2} \qquad (57)$$

4. Derivation of Landauer black hole diameter

$$\begin{aligned} M_{BH}c^2 &= Tk_B \ln(2) \\ \frac{d\ell_P c^2}{4G} c^2 &= \frac{T_P}{2\pi d} k_B \ln(2) \\ \frac{dc^4}{4G}\sqrt{\frac{\hbar G}{c^3}} &= \sqrt{\frac{\hbar c^5}{G k_B^2}} \frac{k_B \ln(2)}{2\pi d} \qquad (58) \\ \frac{d}{2} = \frac{\ln(2)}{\pi d} \quad d &= \pm\sqrt{\frac{\ln(4)}{\pi}} \approx \pm 0.6643 \end{aligned}$$

5. Black hole diameter after absorption or emission of a wavelength l in dimensions n = 2, 3,…,5.

n	$(d_{k+1}^{A/E})^{n-1}$
2	$d_k \pm 8\pi/l$
3	$d_k^2 \pm 16\pi d_k/l + 64\pi^2/l^2$
4	$d_k^3 \pm 24\pi d_k^2/l + 192\pi^2 d_k/l^2 \pm 512\pi^3/l^3$
5	$d_k^4 \pm 32\pi d_k^3/l + 384\pi^2 d_k^2/l^2 \pm 2048\pi^3 d_k/l^3 + 4096\pi^4/l^4$

6. Negative and imaginary unit lengths.

There are four possibilities for the volume of unit n-cubic element r^n in n-dimensional space in dependence on what we take as the unit length $r = \{1, -1, i, -i\}$:

$$r = 1 \quad r^n = 1 \quad n \in \mathbb{C}, \qquad (59)$$

$$r = -1 \quad r^n = \begin{cases} 1 & n \text{ is even} \\ -1 & n \text{ is odd} \\ \mathbb{C} & n \in \mathbb{R}/\mathbb{Z} \cup n \in \mathbb{C} \end{cases}, \qquad (60)$$

$$r = i \quad r^n = \begin{cases} 1 & n = \pm 0, 4, 8, \ldots \\ -1 & n = \pm 2, 6, 10, \ldots \\ i & n = \ldots, -7, -3, 1, 5, 9, \ldots \\ -i & n = \ldots, -9, -5, -1, 3, 7, \ldots \\ \mathbb{C} & n \in \mathbb{R}/\mathbb{Z} \cup n \in \mathbb{C} \end{cases}, \qquad (61)$$

$$r = -i \quad r^n = \begin{cases} 1 & n = \pm 0, 4, 8, \ldots \\ -1 & n = \pm 2, 6, 10, \ldots \\ i & n = \ldots, -9, -5, -1, 3, 7, \ldots. \\ -i & n = \ldots, -7, -3, 1, 5, 9, \ldots \\ \mathbb{C} & n \in \mathbb{R}/\mathbb{Z} \cup n \in \mathbb{C} \end{cases} \qquad (62)$$

Unit length r is just a scaling factor of a relation between vertices of the graph of nature. It can be real (positive or negative), or imaginary (positive or negative). Any vertex out of the countably infinite number of vertices can have any relation with the other vertices. But only real and positive unit length (59) yields real and positive unit n-cubic element r^n for each complex n.